

Electrolyte Dependence of CO₂ Electroreduction: Tetraalkylammonium Ions Are Not Electrocatalysts

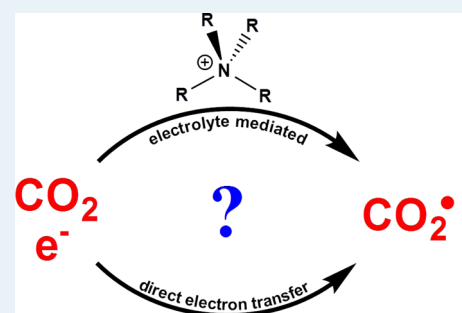
Timothy C. Berto, Linghong Zhang, Robert J. Hamers, and John F. Berry*

Department of Chemistry, University of Wisconsin, 1101 University Avenue, Madison, Wisconsin 53706, United States

Supporting Information

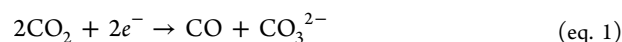
ABSTRACT: The ability of tetraalkylammonium ions (NR₄⁺) to facilitate CO₂ electroreduction at various electrode surfaces has been investigated. Scan rate dependence shows this process to be diffusion-controlled and largely independent of working electrode material. Variation of the R groups on NR₄⁺ is shown to have little effect on the reduction potential, indicating that catalysis via reduced NR₄[•] species, as previously proposed in the literature, is not a viable mechanism for CO₂ electroreduction. Rather, CO₂ is reduced via outer-sphere electron transfer according to the mechanism put forth by Savéant and co-workers [Lamy, E.; Nadjo, L.; Savéant, J.-M. *J. Electroanal. Chem.* 1977, 78, 403–407]. This view is supported by a full analysis of the reaction products, which consist exclusively of CO and CO₃²⁻, as well as solvent decomposition products formed at the counter electrode. No degradation of NR₄⁺ ions is observed, which rules out the transient formation of NR₄[•] radical species during electroreduction. However, Li⁺ ions are definitively shown to inhibit CO₂ reduction, even in the presence of NR₄⁺ ions. This inhibition likely occurs via surface adsorption of the Li⁺ ions.

KEYWORDS: carbon dioxide, electrochemistry, tetraalkylammonium, boron-doped diamond



INTRODUCTION

A large body of current research is devoted to the discovery of alternative fuel sources and the mitigation of greenhouse gas emissions.^{1,2} In particular, electrochemically driven CO₂ reduction to give useful industrial feedstocks provides an attractive blueprint for recycling carbon-based emissions. In this way, CO₂ can be converted to a variety of compounds including carbon monoxide, formaldehyde, methanol, and others. A number of transition-metal-containing catalysts for these reactions have been developed in recent years,^{1–6} with rates of up to 1000–10 000 M⁻¹ s⁻¹ for conversion of CO₂ to CO having been achieved.^{5,7,8} However, it is important to note that CO₂ can be electrochemically or photoelectrochemically reduced to CO in the presence of tetraalkylammonium (NR₄⁺) cations,^{9,10} which are very commonly used as supporting electrolytes and widely believed to be chemically inert. Under proton-limited conditions, these systems typically produce CO with carbonate presumed to be the byproduct via eq. 1:^{11,12}



Tetraalkylammonium salts have been described as CO₂ reduction “catalysts” even though they are always employed in large excess relative to CO₂.^{13,14} The typical mechanism invoked for the observed reactivity involves reduction of NR₄⁺ to give the corresponding neutral radical, which then transfers an electron to CO₂.¹⁵ However, experimental evidence supporting such a mechanism is lacking. In protic solvents, a mixture of several CO₂ reduction products is formed,^{15,16} but in

aprotic solvents, the reaction is claimed to be selective for the production of CO.¹² In order to clarify the mechanistic role of NR₄⁺ species, we explore here electrochemical CO₂ reduction in aprotic solvents under a broad range of conditions with NR₄⁺ cations of variable alkyl chain length as well as complementary experiments utilizing Li⁺ and Cs⁺. Several working electrode materials are tested, including inexpensive boron-doped diamond. Labeling experiments with ¹³CO₂ were also performed to assess unambiguously the product distribution of the reactions.

EXPERIMENTAL SECTION

Research grade CO₂ gas (99.999%) was purchased from Airgas Specialty Gases (Chicago, IL) and was used without further purification. Anhydrous solvents were prepared either by distillation over CaH₂ or via a Vacuum Atmospheres solvent purification system. Anhydrous LiClO₄ and tetrabutylammonium hexafluorophosphate were purchased from Fisher Scientific (Pittsburgh, PA); the latter was dried under vacuum prior to use. All other tetraalkylammonium salts were purchased from GFS Chemical and used without further purification. Boron-doped polycrystalline CVD diamond surfaces were purchased from Element Six and then heated at 800 °C in a 13.56 MHz inductively coupled hydrogen plasma

Received: October 23, 2014

Revised: December 5, 2014

Published: December 9, 2014

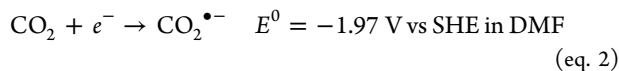
(50 Torr H₂) for 1 h prior to use. Thin-layer diamond on Mo was prepared according to literature methods.¹⁷

Electrochemical measurements were performed using a BAS Epsilon potentiostat connected to a N₂-flushed cell containing 0.25 cm² of exposed surface (working) along with Pt (counter) and Ag (reference) wire electrodes. When necessary, the counter electrode was isolated from the bulk solution via a fine glass frit. Data were not corrected for ohmic drop as the reference electrode was positioned within 1 cm of the working electrode and the electrolyte solutions employed display sufficiently low resistance. FT-IR gas analysis was performed using a 20 cm cell fit with CaF₂ windows mounted in a Bruker Vertex 70 spectrometer. ¹H NMR data were collected on a Bruker 400 MHz Avance spectrometer.

RESULTS AND DISCUSSION

Benchmarking with the Tetrabutylammonium Ion. In order to investigate claims that NR₄⁺ ions catalyze CO₂ reduction, the tetrabutylammonium (NBu₄⁺) ion was used as a benchmark. Here, a 0.25 cm² working electrode was exposed to CO₂-saturated solutions containing 0.1 M NBu₄⁺ as either the hexafluorophosphate or perchlorate salt in an air-free electrochemical cell. It is important to note that the anion present was not found to have any noticeable effect on any electrochemical results. A variety of working electrodes and solvents were also employed under these conditions, as discussed below. Importantly, solution FT-IR data show no interaction between dissolved CO₂ and any NR₄⁺ ions in CH₃CN. For example, Figure S1 shows that the CO₂ stretching vibration remains unchanged in the presence or absence of 0.1 M NMe₄⁺.

Voltammetric analysis in the presence of NBu₄⁺ clearly shows a large current increase beginning at −1.8 V vs Ag/Ag⁺ for CO₂-saturated solutions as compared to a N₂ background (see Figure 1, top). Notably, there are no signals present under N₂ that can be construed as reduction of NBu₄⁺ to NBu₄[•] radical. Under CO₂-limited conditions (2 mL gas injection to 30 mL solvent), an irreversible reductive feature is observed at approximately −2.6 V vs Ag/Ag⁺ during cyclic voltammetry in dry CH₃CN containing NBu₄⁺. This feature is assigned as the formation of CO₂^{•−} according to eq. 2.¹⁸



A plot of the peak current versus (scan rate)^{1/2} shows a linear response for this feature, indicating a diffusion-controlled process (see Figure 1, bottom).

In a further attempt to probe for surface adsorption and adhesion effects, the working electrode material was varied under CO₂-reducing conditions in the presence of NBu₄⁺. Four electrode materials were chosen including platinum, boron-doped conductive diamond, thin-layer diamond on molybdenum, and glassy carbon. As shown in Figure S2, no substantial difference is present in the CO₂ reduction data for each surface. This result is consistent with an outer-sphere electron transfer to CO₂, which does not involve the formation of any strongly surface-bound species.

Analysis of reaction products was performed using a combination of NMR and IR spectroscopy, as well as a PdCl₂ assay that is selective for the presence of CO.¹⁹ Due to the significantly lower amount of product formation during shorter time frame experiments, ¹³CO₂ gas was used to enable efficient NMR analysis of the nonvolatile electrolysis products.

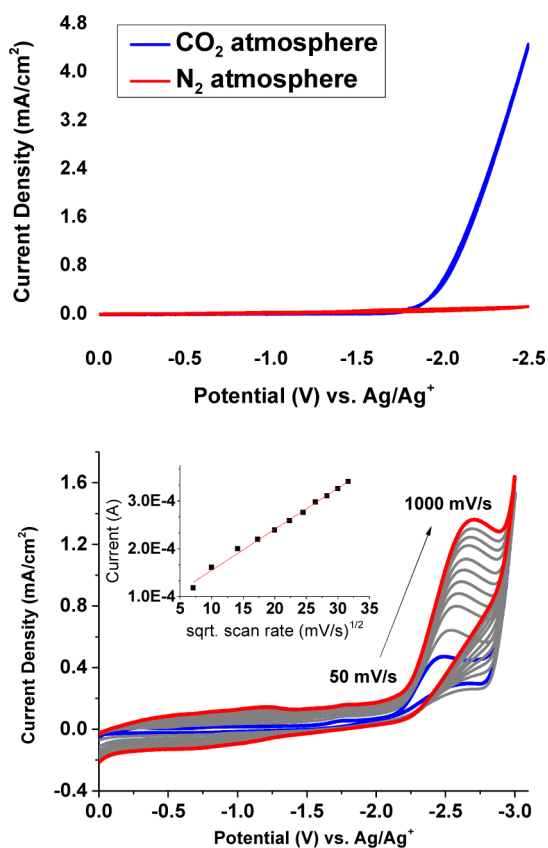
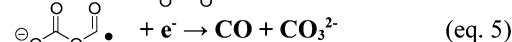
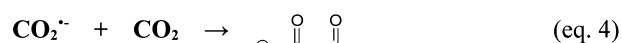
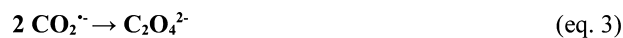


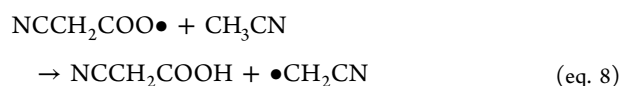
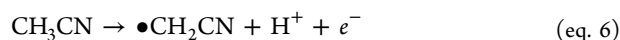
Figure 1. (Top) Cyclic voltammetry recorded at 100 mV/s of CO₂-saturated CH₃CN with 0.1 M NBu₄⁺ as compared to the same solution under N₂. (Bottom) Cyclic voltammetry under CO₂-limited conditions along with a correlation plot showing current vs (scan rate)^{1/2}. All data recorded with a boron-doped diamond working electrode.

When NBu₄⁺ ions were employed during CO₂ reduction in CH₃CN, headspace analysis by PdCl₂ assay reveals production of CO at or near 100% Faradaic efficiency after controlled potential electrolysis (CPE) between −2.1 and −2.6 V. Isotope experiments employing ¹³CO₂ gas lead exclusively to formation of ¹³CO after CPE as evidenced by IR gas analysis (see Figure S3). These results are consistent with a reduction mechanism in which dimerization of the CO₂^{•−} (which would form oxalate as in eq. 3) is suppressed due to high concentrations of neutral CO₂ molecules within the outer Helmholtz plane of the electrode surface. In this way, any CO₂^{•−} produced reacts with neutral CO₂ before it is able to diffuse away from the surface as in eq. 4 and eq. 5.^{6,11,12}



In addition, after long time frame electrolysis (10–24 h) under the above conditions, a yellow/brown precipitate appears at the counter electrode, which is likely NBu₄⁺ cyanoacetate judging by ¹³C NMR and ¹H NMR spectroscopy (see Figures S4 and S5). This side product likely occurs via coupling between NCCH₂[•] produced at the anode via eq. 6 and CO₂ and is only seen upon mixing across the counter electrode frit (see eq. 7 and eq. 8 for the propagation steps of this radical

chain reaction process). Interestingly, CPE performed under identical conditions at 2–3 h time frames shows no indication of cyanoacetate via ^1H or ^{13}C NMR. However, a clear signal for carbonate formation is observed at 168 ppm in the ^{13}C NMR spectrum. Upon continued electrolysis up to 65 h, additional unknown peaks appear in the ^{13}C NMR spectrum at 165 and 155 ppm. Interestingly, these peaks do not show coupling to any signals in the corresponding ^1H NMR spectrum. In fact, no new proton signals are observed at all. Moving away from acetonitrile into DMF solutions greatly clarifies the NMR analysis. Here, only CO is detected as the gaseous product, and only HCO_3^- is observed by ^{13}C NMR. The additional peaks observed when using acetonitrile are therefore attributable to solvent decomposition rather than CO_2 reduction byproducts. The relevant ^1H and ^{13}C NMR spectra are shown in Figures S4–S10.



Finally, to test the hypothesis of diffusion-controlled outer-sphere CO_2 reduction in the presence of NBu_4^+ ions, we decided to investigate the influence of various solvents. For an outer-sphere electron transfer process, the reaction rate (and thus the measured current density) should strongly depend on the properties of the solvent. Due to the large negative potentials required for CO_2 reduction in aprotic media, there are only a handful of solvents that can accommodate the required reaction conditions. For this reason, we chose to use CH_3CN , THF, DMF, and propylene carbonate (PC) to assess the solvent dependence of this reaction. Figure 2 shows cyclic

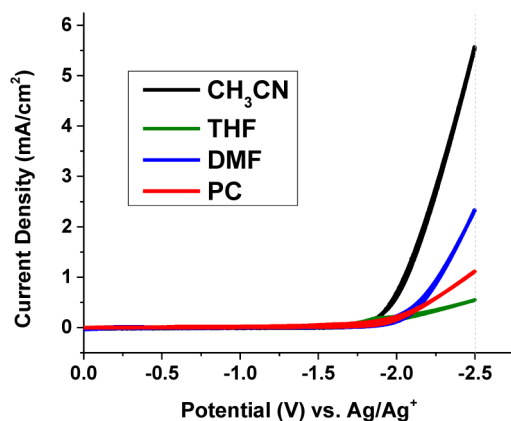


Figure 2. Solvent dependence on CO_2 reduction in the presence of NBu_4^+ . Data recorded at 100 mV/s using a boron-doped diamond working electrode.

voltammograms obtained with H-terminated boron-doped diamond and Pt electrodes in the aforementioned solvents saturated with CO_2 in the presence of 0.1 M NBu_4^+ hexafluorophosphate. These data show acetonitrile to be the optimal solvent choice, giving the largest current at the smallest required potential. THF did not perform well in comparison to the other solvent choices, potentially due to its much lower dielectric constant of 7.58 compared to 36.7 for DMF, 37.5 for CH_3CN , and 64.9 for PC. However, DMF (which has a

dielectric very close to CH_3CN) and PC (which has a much larger dielectric) also performed poorly in relation to CH_3CN .

CO_2 Reduction in the Presence of a Series of NR_4^+ Ions. Given the moderate current densities observed in the presence of NBu_4^+ during CO_2 electroreduction, the investigation of other NR_4^+ salts is warranted. Thus, we chose to look at the effect of varying the alkyl chains between methyl and decyl via addition of the corresponding NR_4^+ salts during electroreduction of CO_2 . As shown in Figure 3, all of the NR_4^+

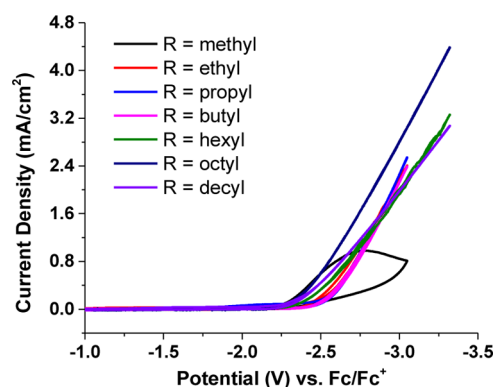


Figure 3. Cyclic voltammetry corrected vs Fc/Fc^+ for CO_2 -saturated solutions containing various NR_4^+ salts at 0.05 M. Data recorded at 100 mV/s using a boron-doped diamond working electrode.

salts tested show reductive current in the presence of CO_2 . Most interestingly, all of the trials, with the exception of NMe_4^+ , show surprisingly similar electrochemical signatures. This is also evident from CPE experiments, although the data are not as straightforward to interpret. Here, CPE data were collected at -2.2 V vs Ag/Ag^+ (Figure S11). However, standardization of the reference potential to ferrocene reveals that the electrolytes with longer alkyl chains appear to alter the Ag wire reference electrode, effectively increasing the “real” applied potential. While the data shown in Figure 3 have been corrected for this discrepancy, indicating no significant difference in the onset of CO_2 reduction with respect to NR_4^+ ion choice, it was not possible to perform such a normalization of the CPE data. Also, due to the incompatibility of an internal ferrocene standard with CO_2 -saturated solutions, all reactions had to be referenced externally to ferrocene, which likely accounts for the small observed spread in onset potentials in Figure 3 due to the reference media not matching exactly that used during CO_2 reduction. We note that NMe_4^+ shows somewhat different behavior from the other electrolytes, showing wave-like behavior in the cyclic voltammogram and a rapid loss of current during CPE. These features are likely due to decomposition of the NMe_4^+ ion during electrolysis.

The series of NR_4^+ ions was also used to allow us to assess the role of the purported $\text{NR}_4\bullet$ radical species as suggested in the literature.^{13,14} Relatively little information is available on the electrochemical reduction of NR_4^+ salt solutions. However, reduction of NR_4^+ salts have been shown to give the corresponding NR_3 amine along with either R_{alkane} or R_{alkene} .^{20,21} The ratio of alkane/alkene formation depends on the nature of the alkyl substituents and the availability of proton donors in solution. Adventitious water and substituents such as ethyl that are more susceptible to Hoffman elimination will favor the alkene. Alternatively, N–C bond cleavage of $\text{NR}_4\bullet$ followed by reduction to give the corresponding carbanion will

favor alkane products. Dahm and Peters have shown that the electrochemical reduction of NEt_4^+ and NBu_4^+ occurs at similar potentials to CO_2 reduction in our system, although we see no evidence to support this under our experimental conditions.²⁰ Not only do we see no electrochemical reduction waves in an atmosphere of N_2 , but no signs of the expected NR_4^+ decomposition products have been observed in our NMR studies. Even after more than 100 C of charge has been passed under a constant potential of -2.2 V vs Ag/Ag^+ in CO_2 -saturated solution, NMR spectra show no indication of either the alkane/alkene or trialkylamine decomposition products of NBu_4^+ , both of which would be expected to form in some quantity after such a long time frame reduction. All told, these data do not support the role of NR_4^+ as a catalyst or even mediator for CO_2 reduction. Only outer-sphere CO_2 electroreduction is observed as has been previously investigated in great detail.^{10,12,18,22}

Inhibition of CO_2 Reduction by Li^+ Ions. In acetonitrile solution, one of the only cation options other than NR_4^+ that is stable under highly reducing conditions is Li^+ . Importantly, essentially no current density is seen under CO_2 -saturated conditions when Li^+ ions are present (0.1 M) in the supporting electrolyte. This is a general trend observed on all working electrode materials tested: glassy carbon, platinum, and boron-doped diamond. These observations have been explained by Li^+ ions inhibiting CO_2 reduction via formation of a hydrophilic layer at the working electrode.^{13,14} Our results are not inconsistent with such an interpretation. Figure 4 shows a comparison of the CO_2 reduction current in the presence of NBu_4^+ ions and lithium ions.

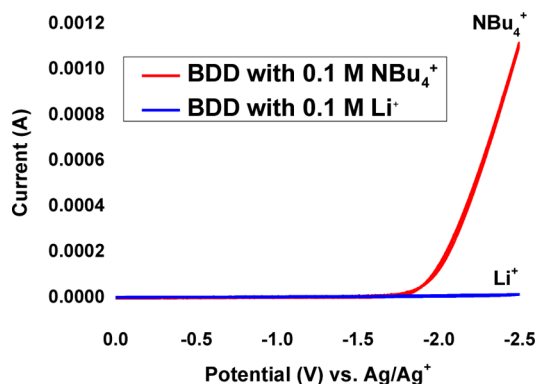


Figure 4. Cyclic voltammetry of CO_2 -saturated CH_3CN in the presence of NBu_4^+ and Li^+ . Data recorded at 100 mV/s using a boron-doped diamond working electrode.

In the case where Li^+ salts are used as the supporting electrolyte, almost no current increase is observed in the presence of CO_2 as compared to inert N_2 gas. Moreover, Li^+ ions are able to effectively arrest CO_2 reduction even in the presence of NR_4^+ electrolytes. Figure S12 shows that, during CPE, the addition of 2 equiv of LiClO_4 (relative to NBu_4^+) to a CO_2 -saturated solution with NBu_4^+ rapidly reduces the current to nearly zero. Conversely, even the addition of large amounts of NBu_4^+ to CO_2 -saturated solutions containing Li^+ does not result in a noticeable current increase. Thus, it appears as though it is the Li^+ ions, and not the NR_4^+ ions, that interact with the electrode surface. Interestingly, the use of CsClO_4 as supporting electrolyte in DMF does show a modest but noteworthy current increase in the presence of CO_2 (see Figure

S13).²³ However, CPE experiments at -2.2 V vs Ag/Ag^+ show a rapid drop in current, very similar to what is observed with NMe_4^+ salts (vide infra). The similar ionic radius of Cs^+ and NMe_4^+ potentially allows similar surface interactions with these two supporting electrolytes.

CONCLUSIONS

Based on the available data, the “catalytic” role of NR_4^+ salts in CO_2 electroreduction is non-existent. None of the current data supports a strong electrostatic interaction between either NR_4^+ and CO_2 or NR_4^+ and the electrode surface, and the diffusion-controlled electroreduction best fits a simple direct outer-sphere reduction of dissolved CO_2 , the mechanism which was originally put forth by Savéant and co-workers.^{18,22} Most importantly, if NR_4^+ ions were involved in catalysis via their corresponding one-electron-reduced radical moiety, the onset of electroreduction should depend greatly on the nature of the R group. This is not the case based on all currently available data. The most likely scenario is therefore that NR_4^+ electrolyte solutions simply do not inhibit outer-sphere CO_2 reduction, whereas Li^+ clearly arrests electroreduction. The observed surface passivation is likely due to either formation of an inhibiting lithium film or to Li^+ adsorption as postulated for photochemical fixation of CO_2 at semiconductor surfaces.²⁴ Here, Lewis acidic Li^+ ions adsorbed at the electrode surface limit CO_2 adsorption and thus inhibit electron transfer. On the other hand, the diffuse charge density on NR_4^+ ions allows for electrochemical contact between CO_2 and the working electrode surface. At this point, it is clear that carbonate is indeed formed alongside CO but can be lost due to the production of H^+ at the counter electrode.

ASSOCIATED CONTENT

Supporting Information

The following file is available free of charge on the ACS Publications website at DOI: 10.1021/cs501641z.

NMR and FT-IR spectra as well as additional voltammetric data (PDF)

AUTHOR INFORMATION

Corresponding Author

*E-mail: berry@chem.wisc.edu.

Notes

The authors declare no competing financial interest.

ACKNOWLEDGMENTS

We thank the University of Wisconsin—Madison and the National Science Foundation (CHE-1300464) for support of this work. Contributions of L.Z. and R.J.H. on diamond electrodes were supported by the Air Force Office of Scientific Research Award FA9550-12-1-0063.

REFERENCES

- (1) Najafabadi, A. T. *Int. J. Energy Res.* **2013**, *37*, 485–499.
- (2) Seyboth, K.; Matschoss, P.; Kadner, S.; Zwickel, T.; Eickemeier, P.; Hansen, G.; Schlomer, S.; von Stechow, C. *Renewable Energy Sources and Climate Change Mitigation*; Cambridge University Press: New York, 2012.
- (3) Costentin, C.; Drouet, S.; Robert, M.; Savéant, J.-M. *Science* **2012**, *338*, 90–94.
- (4) Finn, C.; Schnittger, S.; Yellowlees, L. J.; Love, J. B. *Chem. Commun.* **2012**, *48*, 1392–1399.

- (5) Morris, A. J.; Meyer, G. J.; Fujia, E. *Acc. Chem. Res.* **2009**, *42*, 1983–1994.
- (6) Savéant, J.-M. *Chem. Rev.* **2008**, *108*, 2348–2378.
- (7) Smieja, J. M.; Kubiak, C. P. *Inorg. Chem.* **2010**, *49*, 9283–9289.
- (8) Steffey, B. D.; Curtis, C. J.; DuBois, D. L. *Organometallics* **1995**, *14*, 4937–4943.
- (9) Oh, Y.; Hu, X. *Chem. Soc. Rev.* **2013**, *42*, 2253–2261.
- (10) Taniguchi, I.; Aurian-Blajeni, B.; Bockris, J. O. M. *J. Electroanal. Chem.* **1984**, *161*, 385–388.
- (11) Amatore, C.; Savéant, J.-M. *J. Am. Chem. Soc.* **1981**, *103*, 5021–5023.
- (12) Gennaro, A.; Isse, A. A.; Severin, M.-G.; Vianello, E.; Bhugun, I.; Savéant, J.-M. *J. Chem. Soc., Faraday Trans.* **1996**, *92*, 3963–3968.
- (13) Bockris, J. O. M.; Wass, J. C. J. *Electrochem. Soc.* **1989**, *136*, 2521–2528.
- (14) Saeki, T.; Hashimoto, K.; Kimura, N.; Omata, K.; Fujishima, A. *J. Electroanal. Chem.* **1995**, *390*, 77–82.
- (15) Nakata, K.; Ozaki, T.; Terashima, C.; Fujishima, A.; Einaga, Y. *Angew. Chem., Int. Ed.* **2014**, *53*, 871–874.
- (16) Saha, M. S.; Furuta, T.; Nishiki, Y. *Electrochem. Commun.* **2004**, *6*, 201–204.
- (17) Ramesham, R.; Rose, M. F. *Diamond Relat. Mater.* **1997**, *6*, 17–27.
- (18) Lamy, E.; Nadjó, L.; Savéant, J.-M. *J. Electroanal. Chem.* **1977**, *78*, 403–407.
- (19) Allen, T. H.; Root, W. S. *J. Biol. Chem.* **1955**, *216*, 309–317.
- (20) Dahm, C. E.; Peters, D. G. *J. Electroanal. Chem.* **1996**, *402*, 91–96.
- (21) House, H. O.; Feng, E.; Peet, N. P. *J. Org. Chem.* **1971**, *36*, 2371–2375.
- (22) Savéant, J.-M. *Elements of Molecular and Biomolecular Electrochemistry: An Electro-Chemical Approach to Electron Transfer Chemistry*; John Wiley & Sons: Hoboken, NJ, 2006; pp 152–153.
- (23) The analogous reaction could not be carried out in acetonitrile due to the insolubility of CsClO₄.
- (24) Eggins, B. R.; Robertson, P. K. J.; Murphy, E. P.; Woods, E.; Irvine, J. T. S. *J. Photoch. Photobiol. A* **1998**, *118*, 31–40.